2005 American Control Conference
June 8-10, 2005. Portland, OR, USA

Robust Control and μ analysis of Active Pneumatic Suspension

H.Porumamilla and A. G. Kelkar
Vibroacoustics-Solutions, Inc.
2501 N. Loop Dr., Bldg. 1, Suite 1608
Ames, IA 50011
email: hemanth@iastate.edu, akelkar@vibroacoustics-solutions.com

***Abstract*— This paper presents a novel concept of active pneumatic suspension which uses an accumulator, airspring, and smart control system to actuate a variable orifice mechanism which connects the airspring to the accumulator. The main objective is to obtain a linear model for this pneumatic suspension so as to use existing advanced linear control methodologies to ascertain the closed loop performance and robustness. The two control designs investigated are a robustified LQG and mixed sensitivity H_∞ control. The controllers designed (H_∞ in particular) are shown to provide good performance enhancement over open loop with regard to vibration isolation while guaranteeing a desired degree of robustness to modelling uncertainties.**

I. Introduction

The area of active vehicle suspension has been researched with great enthusiasm for over three decades. Although the benefits of active suspension system are known for several years, such systems are not very common in the present day automobiles, especially in passenger cars. The reason being, the design of active suspension system thought of thus far tends to be economically not viable as the cost, weight, and maintenance considerations outweigh the benefits of comfort. In order for the active suspension design to be practical for passenger cars, its benefits should outweigh its cost and it should exhibit much improved performance and robustness.

Airsprings are widely used on trucks, SUV's and some cars as means to arrest undesirable motion so as to provide a smooth ride. Use of airsprings as an active suspension device is a relatively new concept and has not been thoroughly explored. This study is primarily focused on development of complete linear analytical model and simulation analysis for this linearized active pneumatic suspension. For the purpose of simplicity, the dynamics of the pneumatic suspension system is modelled using a simple 2-DOF quarter car model.

II. Pneumatic Quarter Car Model

Figure 1 shows the schematic of a 2-DOF pneumatic quarter car suspension model. The pneumatic system basically comprises of an airspring, an accumulator and a variable orifice mechanism. A height control valve is also included in the system.

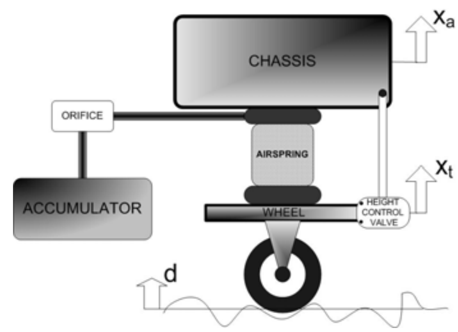

Fig. 1. pneumatic quarter car model

The **airspring** is a sleeve type airbag, which functions as a conventional mechanical spring with the added feature that when used with the height control valve, it maintains a preset optimum design height under varying load conditions thus allowing it to operate in its linear region. The **accumulator** is a large reservoir of air. The main function of the accumulator is to generate additional air volume when vented to the airspring. This additional volume generated causes the pressure in the airspring to drop and hence its stiffness. The **variable orifice mechanism** connecting the airspring with the accumulator establishes the degree of communication between the two and the **height control valve** helps the airspring to operate at a preset optimum design height regardless of the load.

The novelty in the concept proposed is that, as compared to many existing active suspensions, in the present case, the desired vibration isolation is not achieved by introducing external energy, but by

0-7803-9098-9/05/$25.00 ©2005 AACC

intelligently controlling the stiffness of the airspring in real time so as to isolate the suspended mass from undesirable external vibrations. As mentioned above, this change in the airspring stiffness can be accomplished by establishing acoustic communication with the accumulator through a variable orifice mechanism.

A. Linearization

The non-linear equations of motion governing the dynamic behavior of the 2-DOF pneumatic quarter car suspension model are taken from [1] and are as given by Eqns. (1-10).

$$
\begin{aligned}
x_{as} &= (x_{as_o} + x_a - x_t) && (1)\\
p_{as} &= c\left(\frac{a_{as}x_{as}}{m_{as}}\right)^{-\gamma} && (2)\\
m_{acc} &= (m_{total} - m_{as}) \quad p_a = c\left(\frac{V_a}{m_a}\right)^{-\gamma} && (3)\\
\ddot{x_a} &= \left(\frac{p_{as}a_{as}}{m_a}\right) + \frac{C_a}{m_a}(\dot{x_t} - \dot{x_a}) - g && (4)\\
\ddot{x_t} &= \frac{m_a}{m_t}g - \left(\frac{p_{as}a_{as}}{m_t}\right) + \frac{K_t}{m_t}(d - x_t) \\
&+ \frac{C_t}{m_t}(\dot{d} - \dot{x_t}) - \frac{C_a}{m_t}(\dot{x_t} - \dot{x_a}) && (5)\\
\dot{m_{as}} &= \frac{L_1 L_2 L_3}{L_4} && (6)\\
L_1 &= c_d a_o \left(\left[\frac{2g\gamma}{\gamma - 1}\right]\left[\frac{p_{as}m_{as}}{a_{as}x_{as}}\right]\right)^{1/2} && (7)\\
L_2 &= abs\left(\left[\frac{p_a}{p_{as}}\right]^{2/\gamma} - \left[\frac{p_a}{p_{as}}\right]^{\gamma + 1/\gamma}\right) && (8)\\
L_3 &= 1 - \left[\frac{a_o}{a_{as}}\right]^2 \left[\frac{p_a}{p_{as}}\right]^{2/\gamma} && (9)\\
L_4 &= \frac{(p_a - p_{as})}{abs(p_a - p_{as})} && (10)
\end{aligned}
$$

and,
m_a, m_t →mass of the chassis, wheel.
K_t, C_t →stiffness, damping of the wheel.
C_a →airspring damping co-efficient.
x_{as} →height of the airspring.
x_{as_o} →airspring design height(5″).
p_{as}, p_a →airspring, accumulator air pressure.
a_{as}, a_o →airspring, orifice cross sectional area.
m_{as} →mass of air in airspring.
m_{acc} →mass of air in accumulator.
V_a →volume of accumulator.
c_d →orifice discharge co-efficient.
g →acceleration due to gravity.
γ →ratio of specific heat for air.
c →isentropic process constant.

The following rational assumptions are made to aid in linearizing the equations of motion.

The reference point for linearization is chosen to be the steady state condition when the vehicle is moving on flat terrain. In this state, both the chassis and the wheel mass are assumed to have no motion in the vertical direction. Also, their velocities and accelerations in the vertical direction are assumed zero. The cross sectional area of the airspring a_{as} and the design height of the airspring x_{as_o} are assumed to remain constant. The orifice diameter at steady state is 0.75 inch, which means the orifice is half way open. The pressure in the accumulator is assumed to be constant due to its large volume. The term L_3 is approximated to be equal to one. The state variables chosen to obtain the state space representation are,

$$[x_1, x_2, x_3, x_4, x_5] = [x_a, \dot{x_a}, x_t, \dot{x_t}, m_{as}]$$

where,
x_a → absolute displacement of the chassis.
$\dot{x_a}$ → absolute velocity of the chassis.
x_t → absolute displacement of the wheel.
$\dot{x_t}$ → absolute velocity of the wheel.
m_{as} → mass of air in the airspring.
Using these assumptions for linearization and after some algebra, the linearized state space model can be obtained as shown below

$$\Delta\,\dot{x} = [A]\Delta x + [B_u]\Delta a + [B_d]\Delta d \tag{11}$$

$$A = \begin{bmatrix} 0 & 1 & 0 & 0 & 0 \\ Q_1 & -\left[\frac{C_a}{m_a}\right] & -Q_1 & \left[\frac{C_a}{m_a}\right] & Q_2 \\ 0 & 0 & 0 & 1 & 0 \\ P_1 & \left[\frac{C_a}{m_t}\right] & -\left[P_1 + \frac{K_t}{m_t}\right] & -\left[\frac{(C_t + C_a)}{m_t}\right] & P_2 \\ S_1 & 0 & -S_1 & 0 & -S_2 \end{bmatrix}$$

$$B_u = [0, 0, 0, 0, S_3] \qquad B_d = [0, 0, 0, \frac{K_t}{m_t}, 0]$$

The control input to the system is the orifice area Δa and the disturbance input affecting the system is in the form of the road displacement Δd. The model has two performance outputs as mentioned below. These outputs are also measured and used for feedback.

(i) $x_{rel} = (x_t - x_a)$ - the relative displacement between the chassis and the wheel mass, and
(ii) $\ddot{x_a} = (\alpha_a)$ - the acceleration of the chassis.

Hence, the performance output equation then becomes,

$$
\begin{aligned}
y_p &= [C]\Delta x + [D_u]\Delta a + [D_d]\Delta d \qquad (12)\\
C &= \begin{bmatrix} -1 & 0 & 1 & 0 & 0 \\ Q_1 & -\left[\frac{C_a}{m_a}\right] & -Q_1 & \left[\frac{C_a}{m_a}\right] & Q_2 \end{bmatrix}\\
D_u &= [0,0] \qquad D_d = [0,0]
\end{aligned}
$$

The parametric values required to generate the state space matrices are given in tables I and II.

TABLE I

NOMINAL VALUES OF THE SYSTEM PARAMETERS

Q_1 = -175	Q_2 = 6905
P_1 = 1486	P_2 = 58720
S_1 = 60.162	S_2 = 2380, S_3 = 51

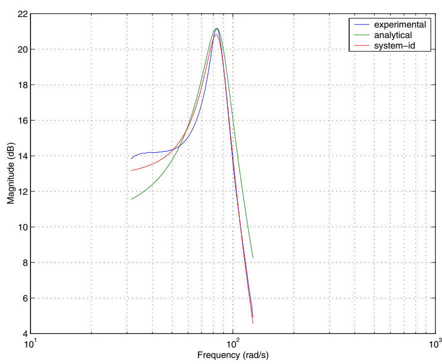

Fig. 2. System identification of wheel parameters

System identification is performed to extract the wheel dynamics with the help of the experimental test rig built so far. From Fig.2, it is evident that both the system identification and analytically obtained transfer functions match very well with the experimental plot. The natural frequency ω_n was found to be approximately 80 rad/s and the damping co-efficient was about 0.16. Hence, from these values of damping co-efficient and natural frequency, the stiffness and the damping constant for the wheel can be easily determined and are as shown in table II.

B. Uncertainty Characterization

The plant uncertainty is assumed to be in the form of parametric variations, i.e., variations in the damping, stiffness, and the mass properties of the system. These parametric variations are modelled using an unstructured output multiplicative uncertainty characterization given in [4]. Table II shows the nominal values of the system parameters and their perturbations considered in this design.

TABLE II

NOMINAL AND PERTURBED PARAMETRIC VALUES FOR THE PNEUMATIC MODEL

Chassis	Tire
M_a =90 ± 10 kg	M_t=16 ±5 kg
K_a =implicit in Eq. of motion	K_t= 1e5 ± 0.1e2 N/m
C_a=50 ± 10 Ns/m	C_t =600 ± 100 Ns/m

The weights obtained for the case of the pneumatic suspension model as as shown in equation set 13.

$$
\begin{aligned}
W_{o_{x_{rel}}} &= \frac{0.08s^4 + 21s^3 + 472s^2 + 577s + 78}{s^4 + 53s^3 + 2987s^2 + 2000s + 2254}\\
W_{o_{\ddot{x}_a}} &= \frac{.2s^6 + 21s^5 + 421s^4 + 442s^3 + 302s^2 + 1.2s + .2}{.6s^6 + 40s^5 + 1400s^4 + 3357s^3 + 5700s^2 + 3700s + 3000}
\end{aligned}
\qquad (13)
$$

The Bode plots of weighting functions in Eq. (13) are shown in Figs. 3 and 4.

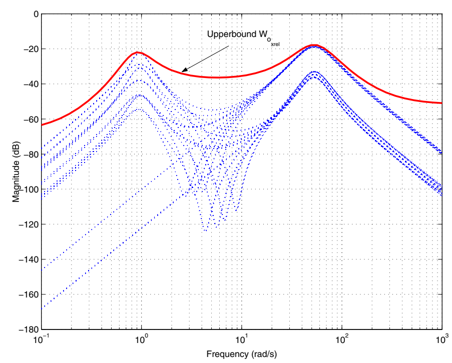

Fig. 3. Uncertainty weight of x_{rel}

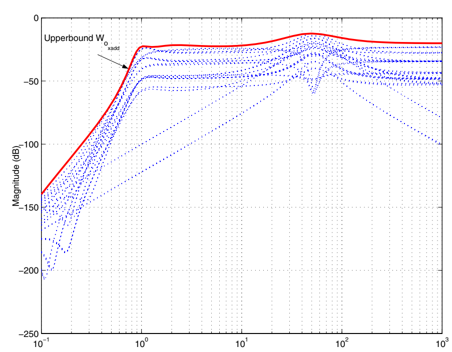

Fig. 4. Uncertainty weight of $\ddot{x}_a$

III. WEIGHTING FUNCTIONS IN THE CASE OF LQG AND H_∞ CONTROLLERS

The selection of weighting functions is highly dependent on the nature of the plant. However, since the pneumatic suspension model has the same essential dynamics as any contemporary suspension model, the weighting functions selected for the present case are not very different from those available in literature [3].

A. Performance Weights

The pneumatic quarter car model considered has three performance outputs. The performance weights for each of the outputs have to be chosen taking into consideration the physical aspects pertaining to that output. Since the nature of the plant does not depend on the type of controller used, the qualitative nature of the weighting functions remains the same. Hence, the weighting functions for the LQG and the H_∞ controller synthesis differ only by DC gain and are provided by the side of each other for easier comparison. The first transfer function for each of the outputs corresponds to the LQG controller.

For the first output, which is x_{rel}, the magnitude of x_{rel} should not be made very small in the low frequency region for safety reasons concerning the handling qualities of the vehicle. At the same time if it is very high, the performance with regards to passenger comfort degrades. Hence, an appropriate low pass filter given by the Eq. (14) is chosen as the performance weight. The H_∞ controller synthesis is able to accept a higher DC gain thereby ensuring tighter control.

$$w_{p_{x_{rel}}} = \frac{1}{s+10}, \qquad \frac{5}{s+10} \tag{14}$$

The second output is the acceleration of the chassis ($\ddot{x_a}$). As explained before, the human body does not appreciate vibrations especially around the 2 Hz region. Hence, in order to suppress the acceleration of the chassis at this frequency, a band pass filter is chosen which provides a notch at the desired frequency of 2 Hz. The transfer function of the filter is given by the Eq. (15).

$$w_{p_{\ddot{x_a}}} = \frac{0.01s}{s^2+7s+40}, \qquad \frac{0.55s}{s^2+7s+40} \tag{15}$$

B. Control Weight

The control weighting is chosen iteratively to be a small constant value of 0.5 in order to satisfy the robust performance constraint explained in [4]. The transfer function is given by Eq. (16).

$$W_u = 0.5, \qquad 5e-6 \tag{16}$$

The H_∞ controller design undertaken in this study is posed as a mixed sensitivity nominal performance problem and uses these performance and uncertainty weights to synthesize an optimal controller. A detailed explanation of the procedure followed is given in [4].

IV. LQG Controller Parameters

The same iterative procedure presented in [4] is used to design a robustified LQG controller. The control design parameters are weighting matrices Q and R and noise covariances V and W. The iterative procedure resulted in the following LQG design parameters for the pneumatic model:

$$\begin{aligned} Q &= \text{diag}\,[1e4,\ 1e8,\ 1,\ 1,\ 1e3]\,; \quad R = [8*1e6] \\ V &= \text{diag}\,[25,\ 0.8]\,; \quad W = [9*1e6] \end{aligned} \tag{17}$$

V. Simulation Results

This section is subdivided into two sub-sections. The first subsection presents simulation results for the case of the nominal quarter car model and the second sub-section presents the perturbation analysis for each of the controllers designed.

A. Performance Analysis

Figure 5 shows the open- and closed-loop bode plots of the chassis acceleration. The main design objective viz Passenger comfort is primarily assessed based on this measure. The open-loop bode plot shows peaks at two frequencies corresponding to the natural frequencies of the chassis approximately (1.0 rad/s) and the wheel approximately (80 rad/s). The closed-loop plot corresponding to the LQG controller is only effective at the Chassis natural frequency. However, the H_∞ controller proves effective at both the critical frequencies. Also, the gain at low frequencies, especially at the natural frequency of the chassis, is considerably lower than that of the LQG controller. Bode plot of the

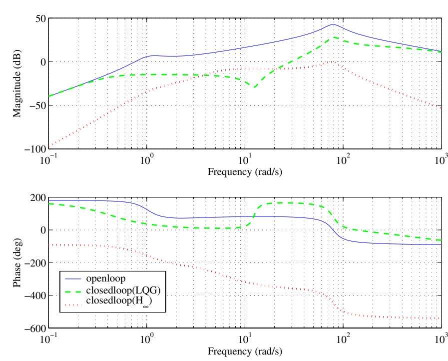

Fig. 5. Bode plots of chassis acceleration $\ddot{x_a}$

suspension space is plotted in Fig. 6. In the case of the LQG controller, even though the controller damps the natural frequency of the chassis, the gain at low frequencies is greatly increased thereby degrading the overall performance. This degradation in performance can be explained as follows; Suspension space and passenger comfort are conflicting demands. The main objective of this research is to improve passenger comfort and hence due to the conflicting nature of the demands, the performance related to suspension space

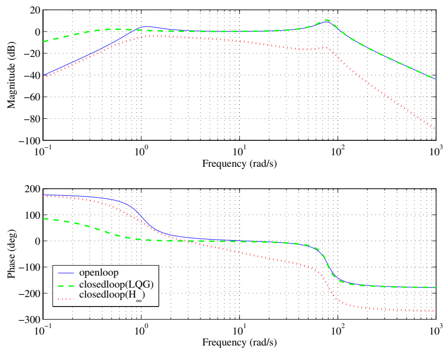

Fig. 6. Bode plots of relative displacement between chassis and wheel x_{rel}

degrades. Even under such conflicting constraints, due to a more advanced and systematic optimization algorithm, the H_∞ controller is able to overcome this inherent compromise and improves the performance of this measure.

Figures 7-8 show the response of the system to an impulse disturbance input. The road disturbance which may be in the form of a bump is modelled as an impulse input with height 3 cms.

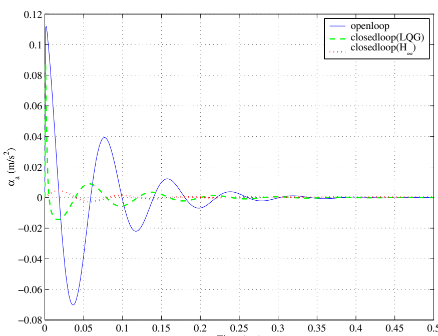

Fig. 7. Impulse disturbance response of chassis acceleration for nominal plant

Figure 7 shows the impulse response of the chassis acceleration. The open-loop has a couple of considerable overshoots apart from the peak overshoot and the settling time is about 0.35 sec. In the case of the LQG controller, even though the settling time has been reduced to about 0.25 and the magnitudes of the overshoots have been reduced, the peak overshoot is almost equal to that of the open-loop. However, in the case of the H_∞ controller, the chassis is almost completely isolated from the disturbance input. All the overshoots including the first overshoot are negligibly small, thereby achieving lower transmissibility.

Figure 8 shows the relative displacement between the chassis and the wheel. As mentioned before, this performance measure signifies road handling capabilities of the automobile. It was shown in Fig. 6, that in the case of the LQG controller, performance of this measure degraded. For safety reasons, it is desired that the road handling

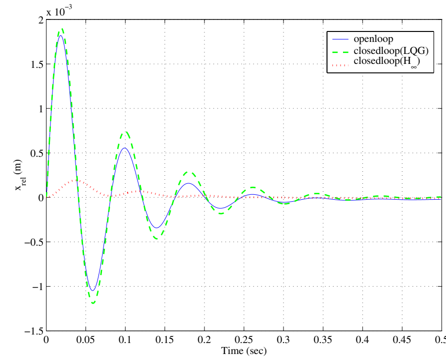

Fig. 8. Impulse disturbance response of Suspension space for nominal plant

feature of the car is not degraded considerably. Hence, to get a better idea of the amount of degradation, time domain analysis is performed. From Fig. 8, it is noticed that the maximum overshoots in the case of the closed-loop system with the LQG controller are about 10 percent higher and the settling time has not been altered drastically as compared to the open-loop. Hence, in the case of the LQG controller, even though there is degradation in performance, it is not alarmingly high. On the contrary, in the case of the H_∞ controller, the performance of this measure is enhanced. Firstly, the magnitude of the peak overshoot has been reduced tenfold. Secondly, the settling time has been reduced from about 0.45 sec to 0.2 sec. Due to the enhancement of this measure, it can be concluded that the compromise between passenger comfort and road handling which was inevitable in the case of the open-loop and the closed-loop with the LQG controller, has been overcome by the H_∞ controller.

As mentioned before, performance enhancement forms only one aspect of design. Another very critical consideration is that of the control effort required. Figure 9 and 10

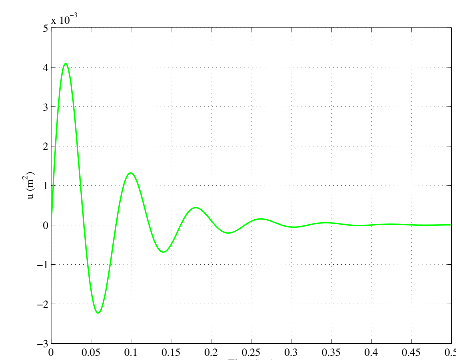

Fig. 9. Control effort in the case of the LQG controller for the nominal plant

show the time history of the control effort for the case of the LQG and the H_∞ controllers respectively. Since, the control input is modelled as an instantaneous change in orifice

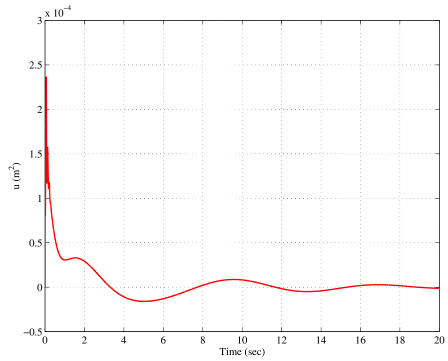

Fig. 10. Control effort in the case of the H_∞ controller for the nominal plant

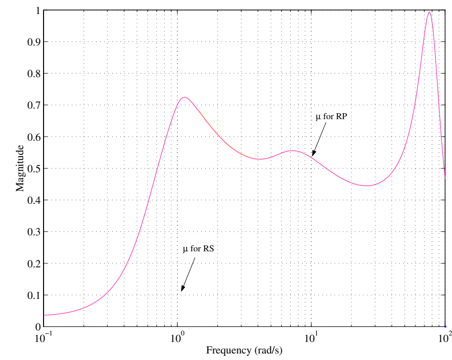

Fig. 12. Structured singular values (μ) in the case of H_∞ controller

area, it can be inferred from the plot that approximately 2.8 inches change in diameter size is demanded by the LQG controller. This is an unacceptably high value which cannot be realized. However, from Fig. 10, the change in orifice diameter required for the case of the H_∞ controller is approximately 0.7 inch. This change in orifice can be more easily achieved and hence, the H_∞ controller appears to be a viable option for hardware implementation.

B. Robustness Analysis

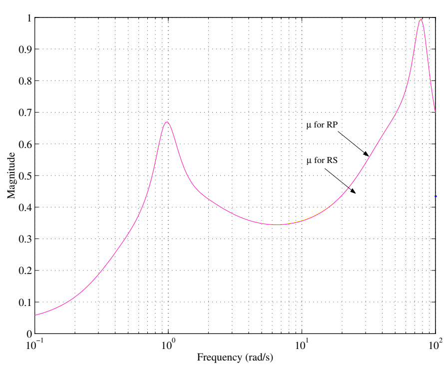

Fig. 11. Structured singular values (μ) in the case of LQG controller

Figure 11 shows the μ for robust stability and robust performance in the case of the LQG controller. The peak magnitude for robust stability and robust performance are strictly less than 1. Hence, it can be concluded that the closed-loop system is not only robustly stable to plant uncertainties but also delivers robust performance in the presence of uncertainty affecting the plant.

A similar result is obtained for the case of the H_∞ controller and is as shown in fig. 12. However, the μ for robust stability in the case of the H_∞ controller is considerably smaller than that for the LQG controller. Since the reciprocal of μ is nothing but the magnitude of uncertainty required to destabilize the system, it can be inferred that the H_∞ controller provides superior robustness.

VI. Conclusions/Future Work

This paper investigates the analytical modelling and linear control design for a novel concept of pneumatic suspension mainly comprising of the airspring, accumulator and a variable orifice mechanism. Unlike contemporary hydraulic suspensions which require addition of energy, the pneumatic suspension relies on intelligently controlling the orifice to provide vibration isolation. The stability robustness and performance obtained as regards to passenger comfort shows an improvement over the open loop. This suggests that the performance of the airsprings which are currently used on many vehicles as passive shock absorbers can be improved by accumulation. The immediate future work will concentrate on the analysis of the nonlinear analytical model through simulation and investigate its behavior as compared to the linearized model studied in this paper. The on-going work will also focus on building an experimental prototype to compliment the analytical study.

Acknowledgements Authors would like to thank Dr. Jerry Vogel, NISUS, Ames, IA 50011 for his suggestions and insights.

References

[1] Vogel J. M. and Claar P. W: “Developement of a slow-active control pneumatic suspension system for heavy vehicle applications.”*SAE Truck and Bus Exposition*, paper No. 912675, 1991.

[2] Claar P. W and Vogel J. M.: “A review of actine suspension control for on- and off- highway vehicles.”*SAE 89C-40, Truck and Bus Exposition*, pp. 6-9, 1989.

[3] Kleinschrodt, T.: “Robust Active Suspension Control Design,” Jun 2001.

[4] Porumamilla, H. and Kelkar, A. G.: “LQG-Based Robust Control of Active Automobile Suspension,” 2003 *ASME International Mechanical Engineering Congress & Expositon*, 2003.

[5] Jeffrey B. B.: “Linear Optimal Control.” *Addison Wesley*, 1999.

[6] Skogestad, S. and Postlethwaite, I.: “Multivariable Feedback Control.” *Wiley*, 1996.